Available online at www.sciencedirect.com

ScienceDirect

Advances in Space Research xxx (xxxx) xxx

ADVANCES IN SPACE RESEARCH (a COSPAR publication)

www.elsevier.com/locate/asr

Magnetic field measurements in a limb solar flare by hydrogen, helium and ionized calcium lines

I.I. Yakovkin [a], A.M. Veronig [b], V.G. Lozitsky [a,*]

[a] Astronomical Observatory of the Taras Shevchenko National University of Kyiv, Observatorna St. 3, Kyiv 04053, Ukraine
[b] Kanzelhöhe Observatory for Solar and Environmental Research & Institute of Physics, University of Graz, 8010 Graz, Universitätsplatz 5, Austria

Received 23 September 2020; received in revised form 24 March 2021; accepted 26 March 2021

Abstract

We present simultaneous magnetic field measurements for the limb solar flare of 1981 July 17 using of the Ca II K, Hδ, He I 4471.5 Å and Hβ lines. For two moments during the flare, which differ in time by 16 min, we analyzed Stokes $I \pm V$ profiles of these lines from observations made on the Echelle spectrograph of the horizontal solar telescope of the Astronomical Observatory of Taras Shevchenko National University of Kiev. At the time step that was close to the peak phase of the flare, all the spectral lines under study showed very wide emissions, with a full width at half maximum (FWHM) of 3.5–4 Å. An interesting feature was observed in the blue wings of these lines, namely, narrow emission peaks with a FWHM of only 0.25–0.35 Å. For heights of 10–18 Mm above the level of the photosphere, we found that (a) very strong kG magnetic fields (up to about 3 kG) existed at both moments of the flare, (b) the locations with strongest fields, in general, do not coincide for different spectral lines, (c) the polarities of the magnetic field for different spectral lines are in most cases identical, but sometimes they do not coincide. The data obtained indicate a significant inhomogeneity of the magnetic field in the flaring corona and the probable presence of the conditions necessary for magnetic reconnection of field lines.

Keywords: Sun; Solar activity; Limb solar flare; Line profiles; Magnetic fields; 'Kilogauss' strengths

1. Introduction

Solar flares occur due to the explosive conversion of free magnetic energy stored in active regions on the Sun into energy in other forms (Priest & Forbes, 2002). As a result of this process, during flares the magnetic energy and magnetic field strength should decrease over time. According to data obtained with solar magnetographs, such decrease is indeed observed (see, e.g., Kosovichev & Zharkova, 1999), but not in all flares.

One of the reasons for this is that solar magnetographs measure the magnetic field not directly by splitting of the magnetically sensitive spectral lines, but by the magnitude of the polarization in the wings of the lines (Babcock, 1953; Scherrer et al., 1995). However, the magnitude of this polarization depends on both the magnetic and non-magnetic changes in the flaring atmosphere. In flares, temperature changes in the flaring atmosphere can be very significant resulting in an appearance of a complex line profile with an emission peak in the cores of some spectral lines (Lozitsky et al., 2018). When measured by a magnetograph, this can give a fictitious value of not only the magnetic field, but also the magnetic polarity (Lozitskaia & Lozitskii, 1982).

Solar flares are interesting in that instead of attenuating the magnetic field in them, the opposite effect can be observed, namely, the maximum field strength occurs in the peak phase of the flare (Lozitsky et al. 2000). Moreover,

* Corresponding author.
E-mail addresses: yakovkinii@gmail.com (I.I. Yakovkin), astrid.veronig@uni-graz.at (A.M. Veronig), lozitsky_v@ukr.net (V.G. Lozitsky).

https://doi.org/10.1016/j.asr.2021.03.036
0273-1177/ 2021 COSPAR. Published by Elsevier B.V. All rights reserved.

the strongest fields are not observed in the lower photosphere, but in the upper photosphere or temperature minimum zone.

The question of the upper limit of the magnetic strength in flares is currently unclear. Especially strong (≥5 kG) magnetic fields in solar flares were firstly suspected by Bruce (1966) and Alikaeva (1970). The author of the former paper supposed that extended wings of the Hα line in flares (up to 8 Å) could arise due to the Zeeman effect in 10–100 kG fields. In fact, this was only one of the possible interpretations, since the observations in unpolarized light were analyzed, i.e., using the Stokes I parameter. In this case, also temperature, turbulent velocity and electric fields should produce some line-profile broadening.

To distinguish these effects the full set of Stokes parameters I, Q, U, and V of the polarized light is needed. On the other hand, if the magnetic field is tangled and unresolved (for instance, in the form of mixed polarity structures) the full-Stokes diagnostics could be useless, because we can essentially detect a broadening of the Stokes I profile but practically zero polarization at different distances from the line center.

It should be noted that the above values of the suspected magnetic field strengths for flares significantly exceed those for sunspots. According to direct observations, the strength of the background field in the sunspot umbra is typically 2–3 kG and only very rarely reaches 5–6 kG (Livingston et al., 2006; Lozitska et al., 2015). However, it should be taken into account that the flare emission occurs mainly above the level in the atmosphere where the magnetic field strength in sunspots is measured. On this basis, theoretically, weaker magnetic fields can be expected here if the structure of the magnetic field in flares is relatively simple, similar to that in sunspots. Only with a certain special topology of the force lines, for example, with their strong twisting, the magnetic fields in flares can be stronger than the usually observed magnetic fields in sunspots (Lozitsky, 2015). Very strong magnetic fields can occur also in a spherical magnetic vortex (Solov'ev, 2013). This is a very interesting and important problem for modern heliophysics which requires additional research, both theoretical and experimental.

Since the local peak of the magnetic field strength in flares was observed in the upper photosphere or even higher (Lozitsky et al., 2000; Lozitsky & Lozitska, 2017), it is interesting to find out whether local concentrations of the magnetic field can be located even higher, namely in the chromosphere and corona. As for the available data, they are still ambiguous. Obviously, the answer to this question requires the comparison of data in spectral lines with different depth of formation as well as the building of semi-empirical flare models. Comparison of direct measurements of the magnetic fields using photospheric and chromospheric lines indicates that the magnetic field in flares measured by splitting of emission peaks in a line core is almost always stronger than the magnetic field measured by splitting of the absorption features outside such peaks for the same line (Harvey, 2012; Lozitsky & Lozitska, 2017). As for the semi-empirical models, they were built using spectral lines with moderate and large Landé factors only and, therefore, they were adapted to the kG field range ($B \sim 10^3$ G). In general, such models lead to an ambiguous picture: in some flares, a local increase in the magnetic field was observed (Lozitsky et al, 2000; Kurochka et al., 2008), while in others the usual monotonic weakening of the magnetic field with height was found (Abramenko and Baranovsky, 2004).

From the point of view of the questions discussed above, flares that occur on the solar limb are of particular interest for several reasons. First, such observations allow direct estimates of heights of the relevant features in the flaring atmosphere, without a reference to a semi-empirical model of the flare. Secondly, in some cases, these heights correspond already to the lower corona, i.e., those layers of the solar atmosphere, where the main energy release of solar flares is likely to occur. Thirdly, limb flares give a simpler spectrum that does not overlap with the Sun's photospheric spectrum. The interpretation of such spectrum does not require the separation of the contributions of the flare itself and the photosphere below the flare. In principle, such separation is possible, but it is based on the construction of a semi-empirical model of the flare, and the latter is always based on certain model assumptions.

To date, there are very little data in the literature about magnetic fields in solar limb flares. The first measurements of this kind were made by Koval (1977) using the Hα line. It was found that the magnitude of the magnetic field, measured by the relative splitting of the line in orthogonal circular polarizations (i.e., in the $I + V$ and $I - V$ spectra, where I and V are the corresponding Stokes parameters), is typically several hundred gauss. However, a case of a rather significant relative displacement of the $I \pm V$ profiles corresponding to a magnetic field strength of 9000 G was also detected (Koval, 1977). Koval (1977) had the following point of view: "However, such large values are unlikely in the light of existing ideas about the structure of magnetic fields in the solar atmosphere". It should be noted that even magnetic fields of $\sim 10^2$ G are 'too strong' for limb flares. Indeed, if the magnetic flux tube is homogeneous and non-twisted, then the upper limit of B_{max} in the tube can be estimated from the simple condition of the equality of the magnetic pressure $B^2/8\pi$ inside the tube and the gas pressure $P = nkT$ outside the tube. Solar limb flares occur in the chromosphere and lower corona, where the gas pressure in the undisturbed atmosphere is $\sim 10^{-1}$–10^2 dyn/cm^2. However, at such pressure, B_{max} should be in range 1–50 G, which is at least an order of magnitude less than observed. Furthermore, given that observations with a circular polarization analyzer give mainly the longitudinal component of the magnetic field, the magnitude of the magnetic field may be even larger. As it was pointed out above, such strong magnetic fields may occur in strongly twisted magnetic structures like force-free flux ropes.

Similar strong magnetic fields were measured also in the X1.2 class limb flare that occurred on 2005 July 14

(Lozitsky & Statsenko, 2006). The obtained results relate mainly to the lower solar corona and correspond to heights of 2–10 Mm above the level of the photosphere. From the measurements by "center of gravity" method for $I \pm V$ profiles of the Hα line, it was concluded that magnetic fields of B = 200–300 G existed at the indicated heights. However, a detailed study of the bisectors of the $I \pm V$ profiles showed that the magnetic field in the flare volume was significantly heterogeneous, which is evident from the fact that the bisectors of the $I \pm V$ profiles were non-parallel. In particular, a local peak of bisector splitting was detected at a considerable distance Δλ from the line core (Δλ ≈ 1.1 Å), which can indicate the presence of very strong magnetic fields of about 10^4 G.

Magnetic fields of 200 G were measured using the Hα line also in the M7.7 limb flare on 2012 July 19 (Kirichek et al., 2013). The results obtained refer to a rather high altitude above the limb, about 40 Mm. In this case, a significant lack of parallelism of the bisectors of the $I \pm V$ profiles was observed too, with a maximum of their splitting at a distance of 0.4 Å from the center of the emission profile. In this study, a theoretical MHD force-free model was proposed that allows to explain an existence of such strong fields in the corona due to the strong twisting of the field lines. According to numerical estimations in the frame of the model, the magnetic field strength increases by about 2 orders in comparison with the weak external field of 1–2 G typical for the solar corona.

Kuridze et al. (2019) reported on unique observations of flaring coronal loops above the solar limb using high-resolution imaging spectropolarimetry in the Ca II 8542 Å line from the Swedish 1 m Solar Telescope. They found magnetic field strengths as high as 350 G at heights up to 25 Mm above the solar limb. This value is similar to the result by Kirichek et al (2013). Microwave and hard X-ray observations of the X8.2 solar limb flare on 2017 September 10 revealed regions of high magnetic field strength (up to 520 G) at projected heights of about 25 Mm (Gary et al., 2018). Kleint (2017) studied chromospheric line-of-sight magnetic field B_{LOS} changes based on spectropolarimetry of the Ca II 8542 Å line obtained with the DST/IBIS instrument during an X1 flare on the solar disk. It was shown that these changes are stronger (<640 Mx cm^{-2}) and appear in larger areas than their photospheric counterparts (<320 Mx cm^{-2}). However, these measurements are difficult to compare with the results discussed above for limb flares, since they relate to significantly lower heights in the atmosphere.

Libbrecht et al. (2019) found magnetic field strengths of 2500 G in a C3.6-class flare, based on the first SST/CRISP spectro-polarimetric observations in the He I D3 line. Because this flare occured on the solar disk, the authors supposed that this strong field existed in the deep chromosphere. A record-breaking coronal magnetic field strengths of about 4000 G in solar active region 12,673 was found by Anfinogentov et al. (2019) using microwave observations. Combining the photospheric vector measurements of the magnetic field and the coronal probing, a nonlinear force-free field coronal model was created, which presents the highest coronal magnetic field strengths reported at various coronal heights.

At present, the variation of the vector magnetic field along structures in the solar corona remains unmeasured. An important step in this direction was made by Schad et al. (2016) using spectropolarimetric data of the He I 10830 Å triplet obtained at the Dunn Solar Telescope with the Facility Infrared Spectropolarimeter. Spectropolarimetric inversions indicate that the magnetic field is generally oriented along the coronal loop axis. Multi-wavelength observations of polarized radio emission in the microwave range also give evidence of strong magnetic fields (up to 1800 G) in the low solar corona above active regions, outside flaring times (Bogod et al., 2012).

Fleishman et al. (2020) presented microwave observations of the X8.2 limb flare on 2017 September 10, demonstrating spatial and temporal changes in the coronal magnetic field. They found that for 2 min during the flare, the field decays at a rate of about 5 Gauss per second, as measured within a flare subvolume of ~ 10^{28} cm^3. This fast rate of decay implies a sufficiently strong electric field to account for the particle acceleration that produces the microwave emission. The decrease in the stored magnetic energy is enough to power the solar flare, including the associated eruption, particle acceleration, and plasma heating. Chen et al. (2020) studied for the same event the coronal magnetic field and the relativistic electrons along the flare current sheet. The measured magnetic field profile reveals a local maximum where the reconnecting field lines of opposite polarities closely approach each other, indicative of the reconnection X-point. A strong reconnection electric field of about 4000 V m^{-1} is inferred near the X-point.

Yadav R. et al (2020) presented high-resolution and multi-line observations of a C2-class solar flare that occurred in NOAA AR 12,740 on May 6, 2019. The rise, peak and decay phases of the flare were recorded continuously and quasi-simultaneously in the Ca II K line with the CHROMIS instrument, the Ca II 8542 Å and Fe I 6173 Å lines with the CRISP instrument at the SST. The temporal analysis of the LOS magnetic field at the flare points exhibits a maximum change of ~ 600 G. After the flare, the LOS magnetic field decreases to the non-flaring value, exhibiting no permanent or step-wise change.

In this paper, we study magnetic fields in an X1.7 class limb flare that occurred 1981 July 17. This event is interesting because its spectra revealed a very narrow spectral component simultaneously with wide spectral emission in the Ca II K, He I 4471.5 Å and hydrogen lines.

2. Observations

The solar flare of 1981 July 17 occurred on the eastern limb of the Sun, at heliographic coordinates (7° S, 90° E). According to the bulletin "Solnechnyie Dannyie" (1981),

the flare was associated with active region No. 325 (this is Hale region No. 17751), which appeared on the Sun's disk on the following day, i.e. 1981 July 18 (Fig. 1).

In Fig. 1, the slanting cross on the left sketch shows the location of the flare on the limb during the initial phase of its development. The small horizontal dash to the left of this cross indicates the location of the entrance slit of our Echelle spectrograph for the first exposure (08:17 UT). Magnetic field intensities (in hundreds of gauss) and magnetic polarities in the sunspots are also shown in Fig. 1.

Fig. 2 shows the flare evolution as observed in the 0.5–4 and 1–8 Å soft X-ray bands by the GOES-2 satellite. The soft X-ray time evolution reveals a double peak behavior of the flare under study, both above X1 level, indicative for two strong episodes of energy release. The first peak as observed in the higher energy GOES channel is centered at 08:09 UT, and the second (higher) peak at 08:18 UT. Also, one can see the long-duration nature of the flare, with the decay of the soft X-ray emission extending over at least 3 h.

From these observations, it follows that the moment 8:17 UT (see below) relates to the maximum of the flare soft X-ray emission, and the moment 8:33 UT to its early decaying phase. Tsuneta et al (1984) classified this flare as SB/X1.7 and wrote: "During 11 min observations the height of the centroid of the hard X-ray source increased by about 5" on the average. The images appear to be an edge-on view of a small loop structure. The photospheric magnetic structure on July 18 and 19 observed with the magnetograph at Kitt Peak (*Solar Geophysical Data*) shows that the neutral line of the active region was nearly parallel to the limb, which is consistent with above interpretation". According to Garcia & McIntosh (1992) and Garcia (1994) this flare had GOES X1.9 class and was classified as high-temperature flare, with a maximum electron temperature $T_{e,max} = 26.6$ MK. In the 21st cycle of solar activity, only eight solar flares had temperatures above 30 MK (the investigated flare on July 17, 1981 also occurred in the 21st cycle). All such flares were observed mainly on the solar disk. Interestingly, in cycle 22, all flares with the indicated highest temperatures were localized only on the eastern and western limbs of the Sun (there were also 8 such flares in total), see Garcia & McIntosh (1992).

The spatial development of the initial phase of the flare can be tracked in the Hα filtergrams recorded at Kanzelhöhe Observatory (Fig. 3). Kanzelhöhe Observatory provides regular high-cadence imaging in the Hα spectral line (Pötzi et al. 2015), and the Hα data back to the year 1973 can be accessed online at the Kanzelhöhe Data archive (http://cesar.kso.ac.at). As one can see from Fig. 3, at 08:05:20 UT the area of the flare ejecta as observed above the limb was almost spherical, with a diameter of about 14 Mm. Approximately 3.5 min later, at 08:08:56 UT, the bright flare volume was extended and reached a height of about 23 Mm. The average velocity of the ascent of the flare apex during this time interval was about 42 km s^{-1}. A significant deviation (about 17°) of the longitudinal axis of the flare from the vertical relative to the limb was also noticeable. Within 4 min, at 08:12:56 UT, the height of the brightest emission of the flare reached 33 Mm, and the average speed of the top ascent decreased to 42 km s^{-1}. However, at this moment, an emission region narrower in cross section was also observed, which had a length of 39 Mm. After another 4 min, at 08:16:56 UT, the height of the brightest emission reached 40 Mm, and the region of narrow emission almost ceased to be visible. In this case, the average velocity of the ascent of the flare apex was even lower, about 29 km s^{-1}. Interestingly, these velocities by the Hα line turn out to be 5–7.5 times greater than the velocities of the X-ray centroid according to Tsuneta et al (1984).

This flare was observed with the Echelle spectrograph of the horizontal solar telescope of the Astronomical Observatory of Taras Shevchenko National University of Kyiv (Lozitsky, 2016), starting from about 08:15 UT. Observers were N.I. Lozitska, V.G. Lozitsky and P.M. Polupan. Natalia Lozitska, identifying the flare position in white light at the entrance slit of the Echelle spectrograph, noticed an interesting detail: this flare was visible for some time also in white light as a small convex feature on Sun's limb. White-light flares observed above the solar limb are rare, and indicative of very high densities in the flare loops.

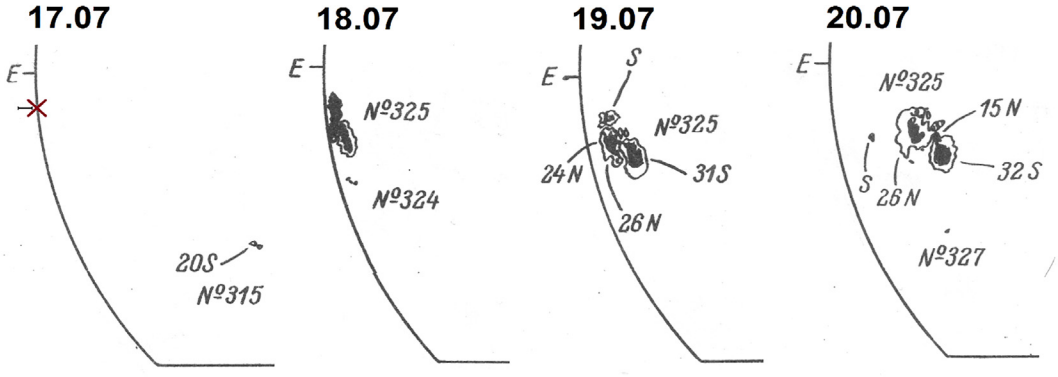

Fig. 1. Sketches of the eastern limb of the Sun for four consecutive days, from July 17 to July 20, 1981, according to the bulletin "Solnechnyie Dannyie". One can see the development of active region No. 325, which was the source of the limb flare under study (see the Text).

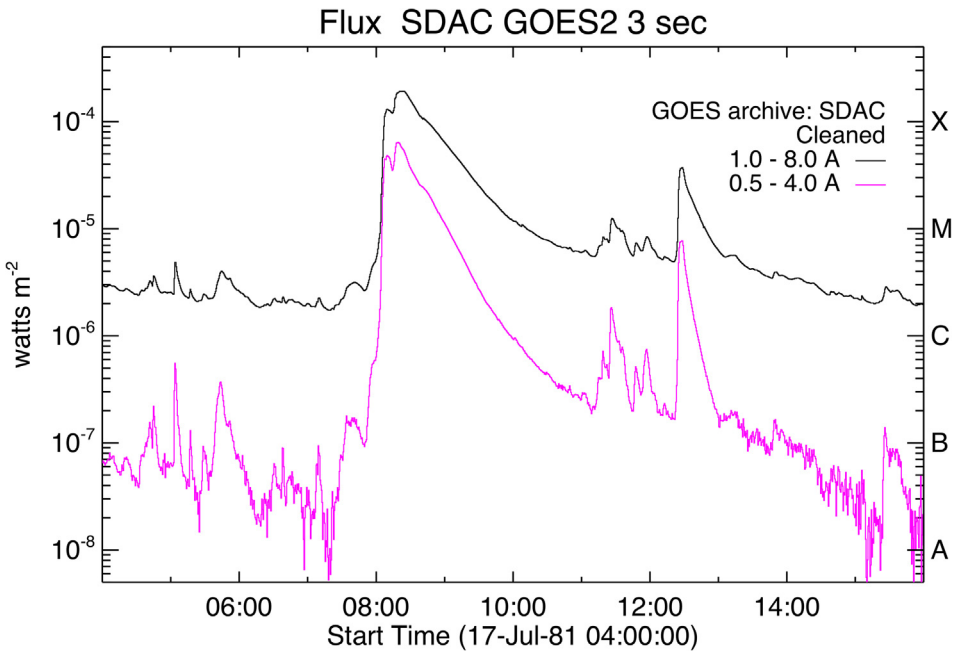

Fig. 2. Soft X-ray flux in the 0.5–4 and 1–8 Å band measured by GOES-2 for the interval 1981 July 17 4:00 UT to 16:00 UT.

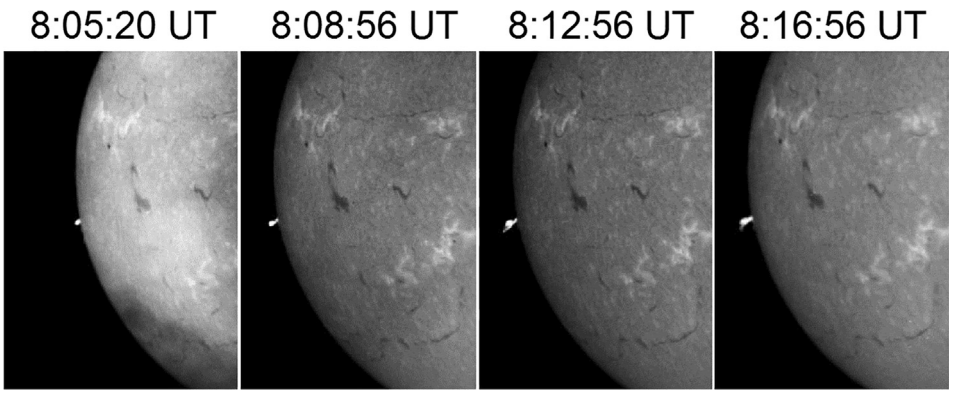

Fig. 3. The development of the initial phase of the flare in Hα heliograms recorded at Kanzelhöhe Observatory (see the Text).

Previous cases were reported and studied by Hiei et al. (1992), You et al. (2003), Saint-Hilaire et al. (2014), Jejčič et al. (2018), etc. Hiei et al. (1992) estimated the electron density in such flare to be in the range of 10^{12}–10^{13} cm^{-3}. Koza et al. (2019) inferred an electron density of 2×10^{12} cm^{-3} in the cool off-limb flare loops of the X8.2 flare on 2017 September 17. The same order of electron density was estimated also for the tops of Hα (post)-flare loops observed in emission against the solar disc (Heinzel and Karlicky, 1987).

The main value of observations with the Echelle spectrograph is that a wide spectrum interval, from 3800 to 6600 Å, was recorded simultaneously where bright and interesting emissions of hydrogen, helium, and ionized calcium lines were observed. Another advantage of such observations is that $I + V$ and $I - V$ spectra were obtained simultaneously, on separate adjacent bands of the spectrograms (see Figs. 4 and 5). This was made thanks to the fact that the circular polarization analyzer consisted of a λ/4 plate in front of the entrance slit of the spectrograph and a beam splitting prism (analogous to the Wollaston prism) behind the entrance slit. Therefore, $I + V$ and $I - V$ spectra relate to the same moment of time and to the same locations on the Sun.

The flare spectrum was photographed on WP1 ORWO photo-plates with exposures of 10–30 sec. In the 08:17–09:51 UT time interval, six exposures were made. Below, two Zeeman spectrograms obtained in 08:17 and 08:33 UT with exposures of 10 and 30 s, respectively, are analyzed.

3. Profiles of spectral lines

A visual inspection of the 08:17 UT spectrogram shows that it contains bright emissions of about ten lines of hydrogen, helium and Ca II. Some parameters of these lines are presented in Table 1 according to Moore (1945)

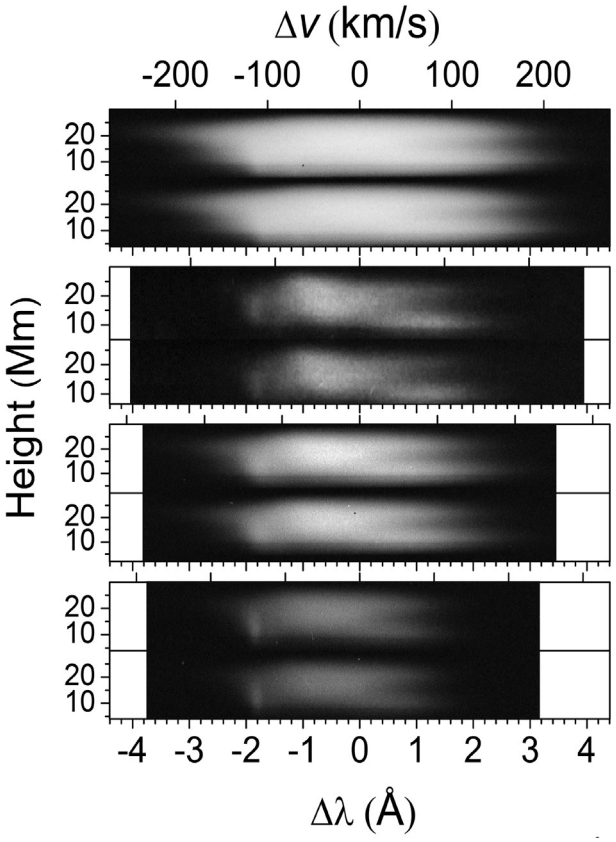

Fig. 4. Spectrograms of the limb flare in the Hβ (top), He I 4471 Å (top middle), Hδ (bottom middle), Ca II K (bottom) lines obtained on 1981 July 17 at 08:17 UT. The top and bottom half of spectrograms correspond to the I–V and $I + V$ spectra, respectively.

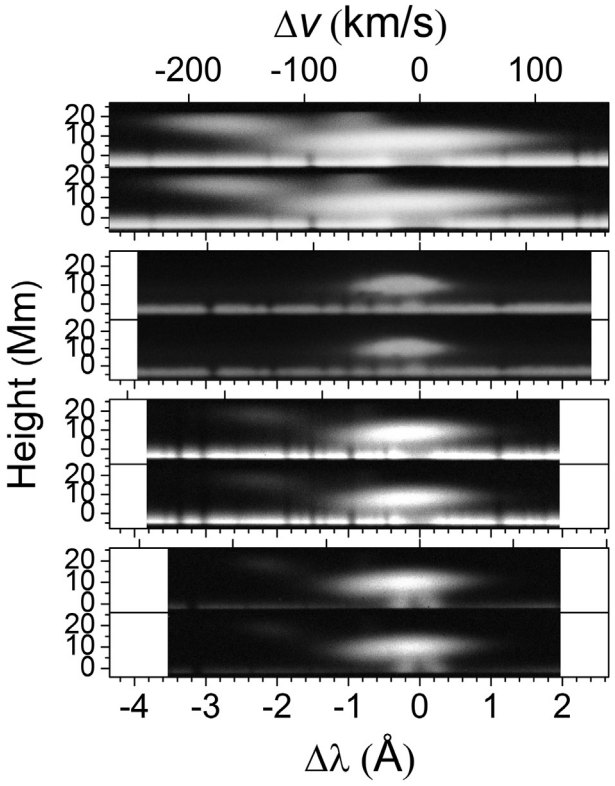

Fig. 5. Spectrograms of limb flare in the lines Hβ (top), He I 4471 Å (top middle), Hδ (bottom middle), Ca II K (bottom) obtained on 1981 July 17 at 08:33 UT. The top and bottom half of spectrograms correspond to the I–V and $I + V$ spectra, respectively. The disk spectrum is visible at the bottom of spectrograms.

and Kurucz & Bell (1995). It is necessary to note that these lines have very different excitation potentials of the lower level, from 0.00 eV to 20.87 eV. Also, the masses of the corresponding atoms are very different, too: about 40 atomic mass unit (m_u) for calcium, 4 m_u for helium and 1 m_u for hydrogen. Therefore, these lines are a suitable tool for diagnostics of turbulent velocities in the flare which needs observations of spectral lines of atoms with very different masses.

The shape of the Ca II K and He I 4471.5 Å lines clearly indicates that there were at least two emission components in these lines: wide and narrow, 1.8–2 Å apart in wavelength (Fig. 4). It can be seen from Fig. 4 that the total widths of the emission lines of Ca II K and Hδ are almost the same. This directly indicates that non-thermal mechanisms play the main role in the broadening of the lines. In case if the profiles of these lines were broadened only by temperature, the width of the Ca II K line would be approximately 6.5 times narrower than the hydrogen line.

At 08:33 UT, i.e., after the peak of the flare, the emissions in the spectral lines split into several discrete components corresponding to a relative line of sight velocities of about 170 km s^{-1} (Fig. 5). The narrow component of the emission has disappeared at this moment and it was not visible even in the Ca II K line. At least three separate emission components are present in the lines under study. These emissions correspond to heights in range of 5–20 Mm above the photosphere.

The measurement of the profiles of these lines was carried out in two ways: by the traditional method using an МФ-4 microdensitometer and using an Epson Perfection V 550 scanner, which allows to obtain two-dimensional scans of images recorded on transparent films or on photo-plates. In the first case, in order to convert the density into intensity, it is necessary to take into account the characteristic curve of the photographic material as well as the scattered light on the photographic plate. In the second case, it is necessary to take into account two characteristic curves, namely, the curve of the photo-emulsion and the curve of the scanner itself. Both curves are nonlinear and require preliminary determination by special methods. In order to do this, we used a step attenuator, for which transmittances are precisely known. As a result, we could compare the data obtained with the microdensitometer and the scanner, and it turned out that these data are very well consistent with each other.

For 08:17 UT, the photometric line profiles clearly show the presence of a discrete narrow component in the blue wing of the observed profiles (Fig. 6). This is most clearly seen in the Ca II K line, where this effect can be traced for about 10 Mm in the slit direction.

Table 1
Spectral line wavelengths and parameters.

Spectral line	Wavelength (Å)	Transition	g_{eff}	Excitation potential (eV)
Hβ	4861.3	$2^2P^0 - 4^2D$	1.05	10.15
He I 4471 Å	4471.5	$^3P_4 - {}^3D_7$	1.12	20.87
Hδ	4101.7	$2^2P^0 - 6^2D$	1.05	10.15
Ca II K	3933.7	$4^2S - 4^2P_0$	1.167	0.00

4. Magnetic fields

4.1. Methods and uncertainties

When measuring the magnetic field by the Zeeman effect, it would be ideal to measure the spectral distance between the lateral orthogonally polarized σ components (i.e. double Zeeman splitting $2\Delta\lambda_H$), ignoring the location of the central π component. This would make it possible to find the modulus of the magnetic field strength, regardless of the orientation of the magnetic field lines. In case such measurement is possible, the influence of scattered light and instrumental polarization can be neglected. When measuring solar magnetic fields, such a unique case happens only in umbra of large sunspots for magnetically sensitive lines with a large Landé factor (about 2.5–3.0) and a narrow spectral width (about 0.1 Å) in the visible spectrum (see, for example, Livingston et al. 2006). Then the Zeeman splitting $\Delta\lambda_H$ can be comparable to the half-width of the spectral line $\Delta\lambda_{1/2}$, so that the Zeeman π and σ components are only slightly blended.

However, the case above does not apply for solar flares. Even for magnetic fields of several kG the spectral width of flare emissions is much larger than the Zeeman splitting (i.e. $\Delta\lambda_H \ll \Delta\lambda_{1/2}$) and therefore the π and σ components are highly blended. In such case the modulus of the magnetic field is unobtainable. Under the assumption that the magnetic field is uniform, the longitudinal component of the magnetic field $B_{LOS} = B\cos(\gamma)$ can be found, where γ is the angle between the field lines and the line of sight. If, however, the magnetic field is two-component in the sense that there are small-scale spatially unresolved flux tubes with the same strengths B and polarities and the filling factor f, embedded in a weaker background field B_{backgr}, then the value close to the product $f\,B_{LOS}$ can be measured from observations (Stenflo, 2011). If, however, the magnetic polarities in spatially unresolved flux tubes are different or the magnetic field in them is close to the transverse orientation ($\gamma \approx 90°$), the measured effective magnetic field B_{eff} can be much lower than the local magnetic field B.

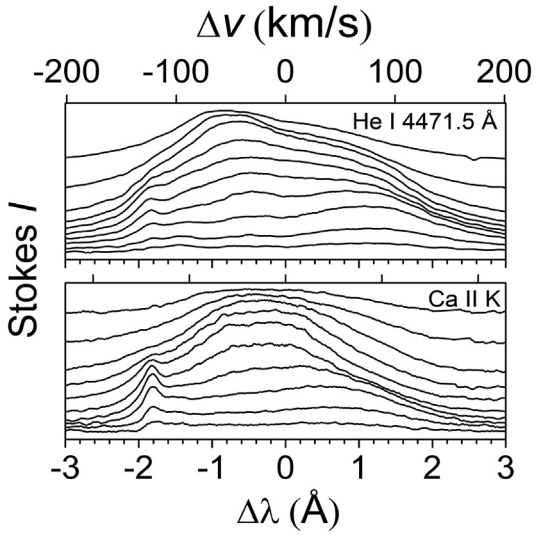

Fig. 6. Stokes I profiles of He I 4471 Å (top) and Ca II K (bottom) lines of the limb flare on 1981 July 17 obtained at 08:17 UT. The profiles correspond to the heights 7.7 Mm (bottom profiles), 10.0 Mm, 12.3 Mm …, and 28.4 Mm (top profiles) above the photosphere.

Therefore, the broad spectral emissions observed in flares make it possible to measure not local magnetic field B, but a certain effective magnetic field B_{eff}, which depends on many parameters, including the algebraic sum of magnetic fluxes of spatially unresolved magnetic elements. Even though the measured value B_{eff} is often very different from the true local magnetic field B, we do believe that B_{eff} has scientific value as it is the lower limit of the local magnetic field since B_{eff} is always lower than B, and in some cases $B_{eff} \ll B$ (Lozitsky et al., 2015). Information even on the lower limit of the magnetic field strengths can be important for elucidating the nature of solar flares, in particular, for constructing better MHD models for them.

The inhomogeneity of magnetic fields in solar flares and prominences follows, at least, from the following spectral effects: (a) the splitting of $I \pm V$ profiles varies from the core to the wings of the emission profiles, generally being larger in the core, and (b) in some cases, the maximum splitting of bisectors of the $I \pm V$ profiles is observed in the wings of the emission profiles, which indicates very strong magnetic fields with complex structures (Harvey, 2012; Kirichek et al., 2013; Lozitsky et al., 2015; Lozitsky & Botygina, 2012). In a uniform magnetic field, the observed splitting of spectral lines should be the same in the line core and its wings.

In the current paper the following different methods were used to measure the effective magnetic field.

Method 1. This method was used for the measurements during the flare peak at 08:17 UT. In frame of this method, the narrow spectral component was explicitly extracted. After this extraction, it was found that the profiles of this component are very symmetrical and can be well fitted by a Gaussian. In this case, it is quite enough to measure the splitting of 'center of gravity' of the whole extracted

profiles. The effective magnetic field $B_{\rm eff}$ was calculated using the following formula:

$$\delta\lambda/2 \ = 4.67 \times 10^{-13} g_{\rm eff} \lambda_0^2 \, B_{\rm eff} \qquad (1)$$

where δλ is observed splitting of $I + V$ and $I - V$ profiles, $g_{\rm eff}$ is the effective Landé factor, λ_0 is the wavelength of the spectral line. In Eq. (1) $B_{\rm eff}$ is expressed in gausses (G) and wavelengths are in Angströms (Å). In case of homogeneous and pure longitudinal field ($\gamma = 0°$ or 180°), $\delta\lambda = 2\Delta\lambda_{\rm H}$. In the opposite case, always $\delta\lambda < 2\Delta\lambda_{\rm H}$.

Probably, the origin of the narrow spectral component is associated with strong magnetic fields of regular polarity, which reduce the stochastic component of the velocity and increase the ordered component corresponding to the circular motions of the plasma around the lines of force. For observations of longitudinal magnetic fields, this should lead to the appearance of narrow spectral lines. From this point of view, a broad component can occur in flare regions with a much weaker magnetic field or in volumes with mixed-polarity fields. In both cases, the Zeeman splitting of the broad component should be observed close to zero. It means that this component can be used as suitable spectral benchmark, i.e., spectral feature with the same wavelength in $I + V$ and $I - V$ spectra.

Method 2. This method was used for the measurements at 8:33 UT. The observed splitting δλ was measured by the "centers of gravity" of the top parts of the emission peaks with intensities in the range from 0.9 to 1.0 of the maximum. The corresponding parameter is denoted below as B_{09}.

In order to evaluate the measurement errors, we used an elegant method proposed by Martinez Gonzalez et al. (2012). For the case of only one spectral line, the corresponding formula (Eq. 17) given in this paper can be written in the form:

$$\delta B_{\rm LOS} = \ \pm \sigma \{ C g_{\rm eff} \lambda_0^2 [\ \Sigma_i (\partial I/\partial\lambda)_i^2]^{1/2} \}^{-1}, \qquad (2)$$

where $\delta B_{\rm LOS}$ is the measurement error, σ is the standard deviation of the corrupting Gaussian noise, $C = 4.67 \times 10^{-13}$ Å^{-1} G^{-1}.

4.2. Measurements

As it was described above, the $I + V$ and $I - V$ spectra were obtained simultaneously, at adjacent places on the spectrogram. In order to measure the Zeeman splittings, these spectra must be scanned separately and then the corresponding line profiles should be 'tied' by wavelengths. The most reliable way to do this is to use telluric or non-magnetically sensitive lines as spectral references with the same wavelength in both orthogonal polarizations. For the limb flare under study, it is quite acceptable to tie the spectra also by the absorption spectrum of the photosphere, if only it hits the photographic plate simultaneously with the flare spectrum.

For 08:17 UT, $I + V$ and $I - V$ profiles were tied to each other by wavelength assuming that their "centers of gravity" coincide in both polarizations. Obviously, the main contribution to the "centers of gravity" was made by the wide emission component, since it is an order of magnitude wider than the narrow component, and the corresponding intensities of the two components are generally commensurate. This linking revealed a reliable splitting of narrow component, which is manifested in the relative displacement of its peaks in the spectra of opposite polarizations (Figs. 7 and 8). Comparing these Figures, it can be seen that the splitting of the narrow component at $\Delta\lambda \approx -1.83$ Å is observed in both lines – He I and Ca II K.

For the measurements taken at 08:33 UT, the "linking" of the profiles was carried out using disk absorption lines, since at that moment the edge of the solar disk was also recorded on the spectrogram (Fig. 5). Such "linking" is more reliable and accurate than for the wide emission component recorded at 08:17 UT.

For both moments of the flare, we found cases when notable Zeeman splitting was observed in not all spectral lines. This illustrates Fig. 9 which shows that although the profiles of both lines correspond to the same place in the picture plane, only in the Ca II K line the splitting of the emission profiles is clearly visible, while in the He I line this effect is absent or much weaker in magnitude. Likely, this effect reflects the fact that different spectral lines formed in different spatial volumes due to different optical depth in these lines. Lines with larger optical depth give us information about the regions of the flare closest to the observer, because quanta from the distant (inner) regions of the flare do not reach the observer. On the contrary, lines with a smaller optical depth provide information on deeper regions of the flare as well. Since it is impossible to expect that all spectral lines have the same optical thickness, some difference in the values of the effective magnetic field strengths is inevitable.

Fig. 9 also implies that in this case, along the line of sight, two luminous volumes of the flare were observed with significantly different Doppler velocities (about 110 km s^{-1}), in which the magnetic polarity was also differ-

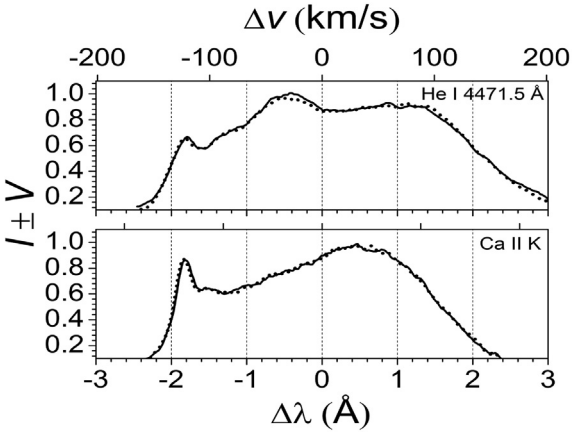

Fig. 7. The I–V (solid) and $I + V$ (dashed) profiles of He I 4471 Å (top, at a height of 14.6 Mm) and Ca II K (bottom, at a height of 12.3 Mm) lines of the limb flare on 1981 July 17 recorded at 08:17 UT.

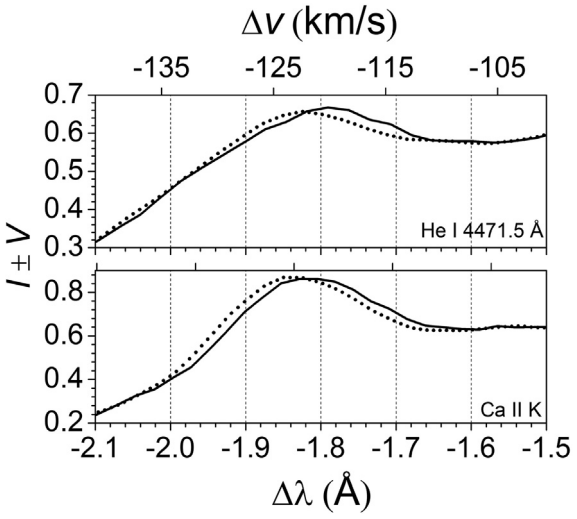

Fig. 8. Details of highly Doppler-shifted profile components (Fig. 6) and the Zeeman split of the *I–V* (solid) and $I + V$ (dashed) profiles.

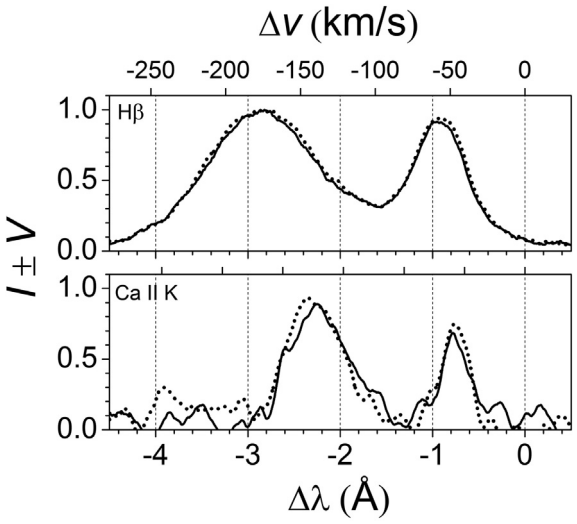

Fig. 9. The *I–V* (solid) and $I + V$ (dashed) profiles of the lines He I 4471 Å (top) and Ca II K (bottom) at a height of 17.9 Mm obtained on 1981 July 17 at 08:33 UT.

ent. According to the measurements, splitting of Ca II K line in left peak ($\Delta\lambda \approx -2.3$ Å) corresponds to magnetic field $B_{09} = 3200$ G (S), whereas in right peak ($\Delta\lambda \approx -0.8$ Å) it corresponds to $B_{09} = 1300$ G (N), where S and N are the corresponding magnetic polarities. The value of B_{09} was found from the splitting of the tops of the emission peaks, as it was described above in *Method 2*.

In order to estimate the measurement error, we take the $(\partial I/\partial\lambda)_i$ values for the Ca II K line with a step of 5 mÅ and assume that in our case $\sigma = 0.01$. Then from Eq. (2) the error is $\delta B_{LOS} = \pm 59$ G. However, this is the lower limit of the probable error in our case. Recall that for the 08:17 UT moment, we were forced to "tie" the $I + V$ and $I - V$ profiles by the "centers of gravity" of the broad emission component, i.e., assume that its Zeeman splitting is zero. This should be true only with a certain accuracy, for example, 100 G. In this case, a more probable error of our measurements can be found as follows: $\Delta B = \pm [(100)^2 + (59)^2]^{1/2} = \pm 115$ G.

From this we can conclude that if the measured field strength in the flare exceeds 1000 G, than the probable error is much smaller than the indicated value itself. Even if we assume that the accuracy of the "linking" of the $I + V$ and $I - V$ profiles by the "centers of gravity" of the broad emission component is 200 G (which seems extremely unlikely), the magnitude of the measured magnetic field B_{LOS} in the flare will be much larger than the measurement errors.

4.3. Results

Our results are summarized in Tables 2 and 3. In these Tables, $\Delta\lambda_H$ presents the Zeeman splitting and B_{eff} (G) the effective magnetic field. These quantities are given for four different height levels above the solar limb, and were obtained by averaging the line profiles over segments corresponding to 2.3 Mm on the Sun in order to obtain a higher signal-to-noise ratio. In these Tables, we present, as rule, only the most reliable data when the values of the measured magnetic fields exceed the measurement errors. For the moment 8:33 UT, two values of the magnetic field for each height are presented, corresponding to the splittings of the left and right emission peaks, as it is shown for example in Fig. 9. For the 8:33 UT moment the He I line had a relatively low intensity, and therefore we omit the corresponding magnetic field measurements.

An examination of Tables 2 and 3 shows the following: (a) very strong kG magnetic fields (till about 3 kG) existed at both moments of the flare, (b) locations with strongest fields, in general, do not coincide for different spectral lines, (c) polarities of the magnetic field for different spectral lines are in most cases the same, but sometimes they do not coincide.

5. Discussion

5.1. Instrumental polarization

The influence of instrumental polarization (IP) as applied to observations with a horizontal solar telescope was discussed earlier by Lozitsky (2016). This discussion is based on the results of studies of this polarization, pre-

Table 2
Comparison of magnetic field strengths in the flare measured at different heights and by different spectral lines. for 08:17 UT.

Line	Height (Mm)	$\Delta\lambda_H$ (mÅ)	B_{eff} (G)
Ca II K	10.0	24.8 ± 1.0	2900 ± 120 (N)
	12.3	10.2 ± 1.0	1200 ± 115 (S)
	14.6	1.3 ± 1.0	150 ± 120 (S)
	16.9	6.2 ± 1.1	750 ± 130 (S)
He I 4471 Å	12.3	2.9 ± 1.4	300 ± 140 (S)
	14.6	15.5 ± 2.1	1500 ± 200 (S)

Table 3
Comparison of magnetic field strengths in the flare measured at different heights and by different spectral lines. for 08:33 UT.

Line	Height (Mm)	$\Delta\lambda_H$ (mÅ) (Left peak)	$\Delta\lambda_H$ (mÅ) (Right peak)	B_{eff} (G) (Left peak)	B_{eff} (G) (Right peak)
Ca II K	11.0	7.7 ± 1.1	7.5 ± 1.0	900 ± 130 (N)	900 ± 125 (N)
	13.3	9.5 ± 1.0	–	1100 ± 110 (S)	–
	15.6	9.9 ± 1.2	5.6 ± 1.1	1150 ± 135 (S)	650 ± 130 (N)
	17.9	27.1 ± 0.9	11.2 ± 1.1	3200 ± 110 (S)	1300 ± 130 (N)
Hβ	13.3	1.3 ± 1.5	–	100 ± 115 (S)	–
	15.6	3.3 ± 1.4	1.2 ± 1.6	300 ± 130 (S)	100 ± 130 (N)
	17.9	3.0 ± 1.4	3.6 ± 1.3	250 ± 120 (S)	300 ± 110 (N)
	20.2	1.3 ± 1.6	1.4 ± 1.8	100 ± 125 (N)	100 ± 130 (N)
Hδ	11.0	4.7 ± 2.0	9.2 ± 1.6	550 ± 230 (S)	1100 ± 190 (N)
	13.3	1.3 ± 1.2	–	150 ± 135 (S)	–
	15.6	9.1 ± 1.1	4.9 ± 1.6	1100 ± 130 (S)	600 ± 190 (N)
	17.9	1.8 ± 1.4	0.3 ± 0.7	200 ± 150 (N)	50 ± 140 (N)

sented in the publications of such authors as Jäger (1972, 1974), Kotov (1973), Grigorjev and Golovko (1975), etc. It was pointed out that for magnetic field measurements on the Sun the best case is modern polarization-free telescope like GREGOR (Schmidt et al., 2012). If, however, we use a telescope of any traditional type, horizontal or tower, we should take into account the main effects occurring due to IP. For a horizontal solar telescope, similar to that in the present study, these are the following.

1. For magnetic field measurements by $I + V$ and $I - V$ profiles, the essential influence of IP occurs due to the linear-to-circular transformation effect (LCT-effect). If linear polarization is zero, the observed $I + V$ and $I - V$ profiles are not distorted by IP. In this case, we can expect an insignificant role of IP for observations of magnetic features with almost longitudinal field ($\gamma = 0°$ or 180°), e.g., for a sunspot near the disc center.
2. IP depends on the angles of reflection on mirrors of a telescope. For instruments with small angles, the value of IP is accordingly smaller. For the Horizontal Solar Telescope of Kyiv Observatory, the largest angles occur on coelostat mirrors. The angles of reflection do not exceed 20°.
3. The phase polarization of the horizontal solar telescope may be approximately presented as an effect of an equivalent phase plate with a path difference equals λ/15–λ/30. The highest phase polarization is observed in the morning and in the evening, and the lowest one in the afternoon.
4. If the observed Zeeman splitting is significantly lower than the spectral half-width of the line ($\Delta\lambda_H \ll \Delta\lambda_{1/2}$), the LCT effect leads to an increase in the depth of the $I + V$ (or $I - V$) profile and to a decrease in the depth of the $I - V$ (or $I + V$) profile, depending on the polarity of the magnetic field. This is due to the fact that, under the LCT effect, both Zeeman σ components give an instrumental circular polarization of the same sign, which is added to the Zeeman circular polarization of different signs in different wings of the magnetically sensitive line. As a result, the observed amplitude of the Stokes V peaks will be different in different wings of spectral line, which causes different depths of the $I - V$ and $I + V$ profiles. However, it is important to emphasize that this does not change the position of the "centers of gravity" of the observed $I + V$ and $I - V$ profiles. That is, the influence of IP does not distort the measurements of longitudinal magnetic fields.

Considering all these effects, we can conclude that the instrumental polarization, apparently, did not have a significant effect on the obtained results. Moreover, we can expect zero influence of instrumental polarization in places with the greatest visible splitting of the spectral lines, where the orientation of the field lines probably corresponds to a purely longitudinal field ($\gamma = 0°$ or 180°), see Section 4.1.

5.2. True magnetic field strength

In principle, the kG magnetic field strengths in the solar limb flare under study do not contradict, in order of magnitude, to some estimates of other authors obtained for approximately the same heights in the corona above active regions. Analyzing the X-ray data for this flare of 17 July 1981, Tsuneta et al (1984) wrote: "In order to confine the hot component in a magnetic tube, the magnetic field strength B must be larger than $B = (24\pi nkT)^{0.5} = 330$ gauss".

Brosius & White (2006) measured the magnetic field of 1750 G at a height of 8000 km above a large sunspot. Reznikova et al. (2009) estimated the field value to be approximately 1 kG in the limb flare loop for the 2002 August 24 event. These estimates follow from the analysis of radio emission under certain model assumptions, i.e., they are not so direct measurements, as our measurements by the Zeeman effect.

It is useful to remember, that similar (and even larger) values were measured in active prominences by Hα and He I D3 lines (Lozitsky & Botygina, 2012). The height range, where such field values were found, is also close in both cases. In the study of Lozitsky & Botygina, (2012), particular attention was drawn to an interesting effect that

has no analogues in the works of other researchers, namely, to the anti-correlation of the magnetic field values derived by the Hα and He I D3 lines, up to their opposite polarity (see their Fig. 5). Thus, it is confirming the earlier conclusion by Yakovkin and Zeldina (1975) that the hydrogen and helium emissions are formed in prominences, in general, in different spatial volumes.

As it was pointed out in Section 4.1, the true values of the local magnetic fields in the flare could be even larger by two reasons: (1) the obtained results represent a longitudinal component of the magnetic field, and (2) it was assumed that filling factor f is close to unity ($f \approx 1$). In case if $f \ll 1$, we can write $B_{\rm eff} \approx f\,B$ where B is true magnetic field strength. Unfortunately, the filling factor f is unknown in our case. Gordovskyy et al. (2018) proposed three different methods for determination of the magnetic filling factor, namely, the magnetic line ratio method, the Stokes V width method, and a simple statistical method. These methods are suitable for the photospheric Fe I 6301.5 Å and 6302.5 Å lines but not for the lines which were studied in our paper.

Our estimates of the magnetic field in the limb solar flare should be considered as some lower limit of the true values of the field intensities. The magnitude of the local magnetic field can be measured either by estimating the filling factor, or by some other special methods independent of this factor. In some cases, it is also possible using the analysis of bisectors of $I \pm V$ profiles (Lozitsky, 2015). This can be done in the future for this flare as a separate study.

Finally, we note that also the visual observation of the arched feature associated with the flare in white light, which is indicated also by the X-ray observations reported in Tsuneta et al. (1984), suggests very high electron density in the flare loops, of the order of 10^{12} cm^{-3} or even higher, as has been recently reported for the high-density flare loops of the 2017 September 10 X8.2 flare (Jejčič et al., 2018; Koza et al. 2019). The arched feature in the flare under study might be of the same nature as the flare loops shown in the HMI continuum images in Figs. 1-3 in Jejčič et al. (2018). High-density flaring plasma implies strong magnetic fields (e.g., Tsuneta et al. 1984). In fact, such strong fields have been measured in the 2017 September 10 flare loops through both microwave diagnostics (Gary et al. 2018, Fleishman et al. 2020) and high-resolution imaging spectropolarimetry by the SST (Kuridze et al. 2019). Thus, the observed arched feature in white light may indicate the presence of strong magnetic field.

6. Conclusion

Investigating two moments of the X1.7 solar limb flare on July 17, 1981, we found interesting features of the emission in Ca II K, Hδ, He I 4471.5 Å and Hβ lines, namely, the simultaneous presence of wide and narrow components in the spectrum during the peak phase of the flare. The observed full width at half maximum (FWHM) of these components differ by about an order of magnitude, 3.5–4 Å and 0.25–0.35 Å, correspondingly. The splitting of the narrow component corresponds to strong magnetic fields as high as 2900 G. During the peak of the flare, the narrow emission component was not detected, and magnetic fields were similar by order of magnitude, up to 3200 G. Such kG magnetic fields were detected at heights of 10–18 Mm. The locations in the picture plane with strongest fields, in general, do not coincide for different spectral lines, whereas magnetic polarities are in most cases the same, but sometimes they do not coincide, which may be a reflection of the magnetic field inhomogeneity. Likely, the true local magnetic fields in the flare could be even larger, since the obtained results represent a longitudinal component of the magnetic field assuming that the filling factor equals unity.

Declaration of Competing Interest

The authors declare that they have no known competing financial interests or personal relationships that could have appeared to influence the work reported in this paper.

Acknowledgements

The authors are grateful to unknown reviewers for useful advices and critical comments. Also, the authors are grateful to Dr. Natalia Lozitska for participating in obtaining valuable observational material and for discussing the results. This study was funded by the Taras Shevchenko National University of Kyiv, project No. 19БФ023-03.

Declaration of Competing Interest

The authors declare that they have no conflict of interest.

References

Abramenko, V.I., Baranovsky, E.A., 2004. Flare-related changes in the profiles of six photospheric spectral lines. Solar Phys. 220, 81–91.

Alikaeva, K.V., 1970. The Zeeman effect in metallic lines of solar flares. Astrometr. Astrofiz. 8, 92–95.

Anfinogentov S.A., Stupishin A.G., Mysh'akov I.I., Fleishman G.D., 2019. Record-breaking coronal magnetic field in solar active region 12673. The Astrophys. J. Lett. 880, article id. L29, 5 pp.

Babcock, H.W., 1953. The solar magnetograph. Astrophys. J. 118, 387–396.

Bogod, V.M., Stupishin, A.G., Yasnov, L.V., 2012. On magnetic fields of active regions at coronal heights. Solar Phys. 276, 61–73.

Brosius, J.W., White, S.M., 2006. Radio measurements of the height of strong coronal magnetic fields above sunspots at the solar limb. Astrophys. J. 641, L69–L72.

Bruce, C.E.R., 1966. Magnetic fields in solar flares. Observatory. 86, 82.

Byull. Solnech. Dannye Akad. Nauk USSR, 1981,7.

Chen, B., Shen, C., Gary, D.E., Reeves, K.K., et al., 2020. Measurement of magnetic field and relativistic electrons along a solar flare current sheet. Nat. Astron. 4, 1140–1147.

Fleishman, G.D., Gary, D.E., Chen, B., Kuroda, N., Yu, S., Nita, G.M., 2020. Decay of the coronal magnetic field can release sufficient energy to power a solar flare. Science 367, 278–280.

Garcia, H.A., 1994. Temperature and emission measure from GOES soft X-ray measurements. Solar Phys. 154, 275–308.
Garcia, H.A., McIntosh, P.S., 1992. High-temperature flares observed in broadband soft X-rays. Solar Phys. 141, 109–126.
Gary D.E., Chen B., Dennis B.R., Fleishman G.D. et al., 2018. Microwave and hard X-ray observations of the 2017 September 10 solar limb flare. The Astrophys. J. 863, article id. 83, 9 pp.
Gordovskyy, M., Shelyag S., Browning P.K., Lozitsky V.G, 2018. Analysis of unresolved photospheric magnetic field structure using Fe I 6301 and 6302 lines. Astron. Astrophys. 619, id. A164, 10 pp.
Grigorjev V.M., Golovko A.A., 1975. A study of the instrumental phase polarization of the horizontal solar telescope. Solnechnyje Dannyje, No. 8, 78–85.
Harvey, J.W., 2012. Chromospheric magnetic field measurements in a flare and an active region filament. Solar Phys. 280, 69–81.
Heinzel, P., Karlicky, M., 1987. Hα diagnostics of (post)-flare loops based on narrow-band filtergram observations. Solar Phys. 110, 343–357.
Hiei, E., Nakagomi, Y., Takuma, H., 1992. White-light flare observed at the solar limb. Publ. Astron. Soc. Jpn. 44, 55–62.
Jäger, F.W., 1972. Instrumental polarization concerning magnetographic measurements. I. Solar Phys. 27 (2), 481–488.
Jäger, F.W., 1974. Instrumental polarization concerning magnetographic measurements II. Solar Phys. 29 (2), 499–508.
Jejčič, S., Kleint L., Heinzel, P., 2018. High-density off-limb flare loops observed by SDO. The Astrophys. J. 867, article id. 134, 10 pp.
Kirichek E.A., Solov'ev A.A., Lozitskaya N.I., Lozitskii V.G., 2013. Magnetic fields in a limb flare on July 19, 2012. Geomagn. and Aeronomy. 53, 831–834.
Kleint, L., 2017. First detection of chromospheric magnetic field changes during an X1-Flare. Astrophys. J. 834, art. id. 26, 10 pp.
Kosovichev, A.G., Zharkova, V.V., 1999. Variations of photospheric magnetic field associated with flares and CMEs. Solar Phys. 190, 459–466.
Kotov, V.A., 1973. On the influence of instrumental polarization on magnetic field measurements. Izv. Krymskoj Astrofiz. Obs. 48, 78–84.
Koval, A.N., 1977. On the measurement of magnetic fields in prominences and flares by the photographic method. Bull. Crimean Astrophys. Obs. 57, 133–143.
Koza, J., Kuridze, D., Heinzel, P. et al., 2019. Spectral diagnostics of cool flare loops observed by the SST. I. Inversion of the Ca II 8542 Å and Hβ lines. The Astrophys. J. 885, article id. 154, 13 pp.
Kuridze D., Mathioudakis M., Morgan H., Oliver R., et al., 2019. Mapping the magnetic field of flare coronal loops. Astrophys. J. 874, art. id. 126, 12 pp.
Kurochka, E.V., Lozitsky, V.G., Osyka, O.B., 2008. Temporal changes of physical conditions in the photospheric layers of a solar flare. Kinemat. Phys. Celestial Bodies 24, 215–222.
Kurucz R.L., Bell B., 1995, Atomic Line Data, Kurucz CD-ROM No. 23. Cambridge, Mass.: Smithsonian Astrophys. Obs., https://www.cfa.harvard.edu/amp/ampdata/kurucz23 /sekur.html.
Libbrecht T., de la Cruz Rodriguez J., Danilovic S., Leenaarts J. et al., 2019. Chromospheric condensations and magnetic field in a C3.6-class flare studied via He I D3 spectro-polarimetry. Astron. Astrophys. 621, id.A35, 21 pp.
Livingston, W., Harvey, J.W., Malanushenko, O.V., 2006. Sunspots with the strongest magnetic fields. Solar Phys. 239, 41–68.
Lozitska, N.I., Lozitsky, V.G., Andryeyeva, O.A., Akhtemov, Z.S., et al., 2015. Methodical problems of magnetic field measurements in umbra of sunspots. Adv. Space Res. 55, 897–907.
Lozitskaia, N.I., Lozitskii, V.G., 1982. Do "magnetic transients" exist in solar flares?. Soviet Astron Letters. 8, 270–272.
Lozitsky, V., Lozitska, N., 2017. Comparison of chromospheric and photospheric magnetic fields in two solar flares of X1.1/4N and X17.2/4B importance. Bull. of Taras Shevchenko National University of Kyiv. 56, 47–51.
Lozitsky V., Masliukh V., Botygina O., 2015. Estimations of local magnetic fields in prominences which have great optical thickness in emissive elements. Bull. of Taras Shevchenko Nat. Univ. of Kyiv. Astronomy. 52, 7–11.
Lozitsky, V.G., 2015. Small-scale magnetic field diagnostics in solar flares using bisectors of $I \pm V$ profiles. Adv. Space Res. 55, 958–967.
Lozitsky, V.G., 2016. Indications of 8-kilogauss magnetic field existence in the sunspot umbra. Adv. Space Res. 57, 398–407.
Lozitsky, V.G., Baranovsky, E.A., Lozitska, N.I., Leiko, U.M., 2000. Observations of magnetic field evolution in a solar flare. Solar Phys. 191, 171–183.
Lozitsky V.G., Baranovsky E.A., Lozitska N.I., Tarashchuk V.P., 2018. Profiles of spectral lines, magnetic fields and thermodynamical conditions in X17.2/4B solar flare of October 28, 2003. Monthly Notices of the Royal Astron. Society. 477, 2796–2803.
Lozitsky, V.G., Botygina, O.A., 2012. Comparison of the magnetic fields in active prominences measured from HeI D_3 and Hά lines. Astron. Lett. 38, 380–387.
Lozitsky V.G., Statsenko M.M., 2006, Proc. of 3rd Int. Scient. Semin. "Physics of the Sun and stars", Elista, Kalmyk Univ., 29 May-2 June 2006, 43–50.
Martínez González M. J., Manso Sainz R., Asensio Ramos A., Belluzzi L., 2012. Analytical maximum likelihood estimation of stellar magnetic fields. Monthly Notices of the Royal Astron. Society. 419, 153–163.
Moore C.E., 1945. A multiplet tables of astrophysical interest. Revised edition. Part I – Table of multiplets // Contributions from the Princeton University Observatory. 20, 110 p.
Pötzi, W., Veronig, A.M., Riegler, G., Amerstorfer, U., et al., 2015. Real-time flare detection in ground-based Hα imaging at Kanzelhöhe Observatory. Solar Phys. 290, 951–977.
Priest, E.R., Forbes, T.G., 2002. The magnetic nature of solar flares. Astron. Astrophys. Review. 10, 313–377.
Reznikova, V.E., Melnikov, V.E., Shibasaki, K., et al., 2009. 2002 August 24 limb flare loop: dynamics of microwave brightness distribution. Astrophys. J. 697, 735–746.
Saint-Hilaire P., Schou J., Martinez Oliveros, J.-C., Hudson H.S., Krucker S., Bain H., Couvidat S. 2014. Observations of linear polarization in a solar coronal loop prominence system observed near 6173 Å. The Astrophys. J. Lett. 786, Iss. 2, article id. L19, 5 pp.
Schad T.A., Penn M.J., Lin H., Judge P.G., 2016. Vector magnetic field measurements along a cooled stereo-imaged coronal loop. The Astrophys. J. 833, article id. 5, 16 pp.
Scherrer, P.H., Bogart, R.S., Bush, R.I., et al., 1995. The solar oscillations investigation - Michelson Doppler imager. Sol. Phys. 162, 129–188.
Schmidt, W., von der Lühe, O., Volkmer, R., Denker, C., et al., 2012. The 1.5 meter solar telescope GREGOR. Astron. Nachrichten 333 (9), 796–809.
Solov'ev, A.A.,, 2013. Spherical magnetic vortex in an external potential field: a dissipative contraction. Solar Phys. 286, 441–451.
Stenflo, J.O., 2011. Collapsed, uncollapsed, and hidden magnetic flux on the quiet Sun. Astron. & Astrophys., 529, id. A42, 20 pp.
Tsuneta, S., Nitta, N., Takakura, T., Makishima, K., et al., 1984. Hard X-ray imaging observations of solar hot thermal flares with the HINOTORI spacecraft. Astrophys. J. 284, 827–832.
Yadav R., Baso C.J.D., da la Cruz Rodríguez J., Calvo F., 2020. Stratification of physical parameters in a C-class solar flare using multi-line observations. eprint arXiv:2011.02953.
Yakovkin, N.A., Zeldina, M.Yu., 1975. The prominence radiation theory. Solar Phys. 45, 319–338.
You, J., Hiei, E., Li, H., 2003. The white-light limb flare of 16 August 1989 and its chromospheric counterpart. Solar Phys. 217, 235–245.